H. De Gersem, B. Renier, K. Hameyer, R. Belmans, "The linear induction motor, a useful model for examining finite element methods on general induction machines", Symposium on power electronics, industrial drives, power quality, traction systems (Speedam), Capri, Italy, June 5-7 1996, pp. A7-7-A7-14.

The Linear Induction Motor, a Useful Model for examining Finite Element Methods on General Induction Machines

Herbert De Gersem, Bruno Renier, Kay Hameyer and Ronnie Belmans

Katholieke Universiteit Leuven
E.E. Dept., Div. ESAT/ELEN
Kardinaal Mercierlaan 94, B-3001 Leuven - Heverlee, Belgium

Abstract
The paper illustrates the use of a linear induction motor as a benchmark model for electromagnetic calculation and simulation of induction motor behaviour. A sequence of operations is set up in order to derive machine parameters for dynamic simulation. The properties of the model allow both analytical and empirical controls during the whole calculation process.

1. INTRODUCTION

Nowadays, the design and study of electrical machines require accurate methods, due to the increasing importance of secondary phenomena as saturation, vibrations and audible noise. The designer has to dispose of powerful calculation and simulation methods in order to design a machine satisfying the requirements with minimal unwanted and undesirable side effects. Also optimizing motor models supposes some knowledge on eventual conceptual and geometric changes on the model and their influences on both steady state and dynamic motor behaviour. For research on improved calculation and simulation methods on induction machines, a reduced induction motor model is required.

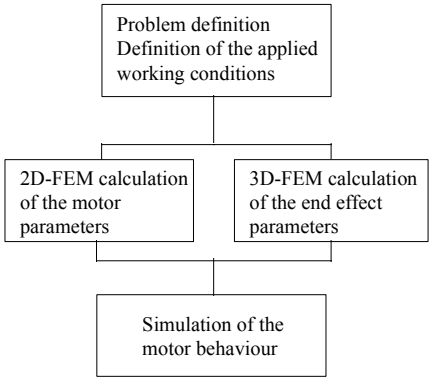

Figure 1 : Flow chart of sequential operations

This paper proposes a linear induction motor as a benchmark model [1]. The considered calculation methods are two- and three-dimensional finite element methods. As a simulation model the coupled inductor model is used. The sequence of operations is shown in figure 1.

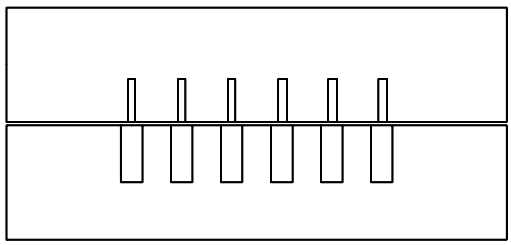

Figure 2 : Linear motor

2. THE LINEAR MOTOR

The development of numerical methods for analysis of electrical machines is impossible without the comparison of both analytical and empirical data. During operation, the cylindrical induction motor does not give the possibility to measure rotor quantities, ohmic resistance and rotor flux. To overcome these difficulties and to provide a distincted and easy model for calculations, a linear induction motor is used.
A linear motor (figure 2) consisting of six stator slots and six rotor slots, two times three stator windings and six

rotor bars can be externally connected in several different ways. The advantages of the model are

1. possibility of measuring both on stator and rotor,
2. freedom of changing stator and especially rotor configuration,
3. facility of the analytical calculation of motor parameters and
4. interesting motion end effects of stator and rotor [2].

The last topic is not the subject of this investigation.

The concept of the linear motor makes it possible to apply exotic configurations and working conditions on stator and rotor, as their are bar and end ring fractions, insulation faults in stator windings, extra external impedances, asymmetric height of the air gap.

3. COUPLED INDUCTOR MODEL

The differential equation

$$[U] = \frac{d[\psi]}{dt} + [R].[I] \qquad (1)$$

describes the behaviour of the three stator phases and the six rotor phases of the linear motor. The resistance matrix [R] is a diagonal matrix with the resistance values of each phase. The values are supposed to be time-independent. The flux matrix [ψ] can be written as

$$[\psi] = [L].[I] \qquad (2)$$

with [I] the matrix of the phase currents and [L] the inductance matrix. The diagonal elements of [L] are the self inductances of the phases. The other elements are the mutual inductances between the phases. [L] is a symmetric matrix. Because of the motion of the geometry and the saturation in the iron, [L] is time-dependent.

When neither motion nor saturation is taken into account, the behaviour of a voltage driven induction motor is described by a set of first order differential equations representing a linear system:

$$[U] = [L].\frac{d[I]}{dt} + [R].[I] \qquad (3)$$

When the time-dependency of [L] has to be concerned, it is for numerical reasons better to consider the equivalent equation [4]:

$$\frac{d[\psi(t)]}{dt} = [U(t)] - [R].[L(t)]^{-1}.[\psi(t)] \qquad (4)$$

This nonlinear differential equation is being solved by a automatic step size Runge-Kutta-Fehlberg integration method [3]. Another possibility is a solution based on a time stepping method combined with a Newton-Raphson iteration.

4. 2D FINITE ELEMENT CALCULATION OF THE MOTOR PARAMETERS

The inductance matrix for the coupled inductor model is calculated by a two-dimensional finite element method. A flow chart is given in figure 3. A detail of the two-dimensional mesh is given in figure 4.

4.1. Influence of saturation

The inductance values in [L] depend on the saturation in the machine. The level and the places of saturation depend on the applied working conditions of the linear motor and on the instant time. Working conditions are both the way of connecting stator windings and rotor bars and the way of exciting the machine. In order to obtain the time varying inductance matrix, a calculation of the magnetic reluctivities at each time step has to be performed.

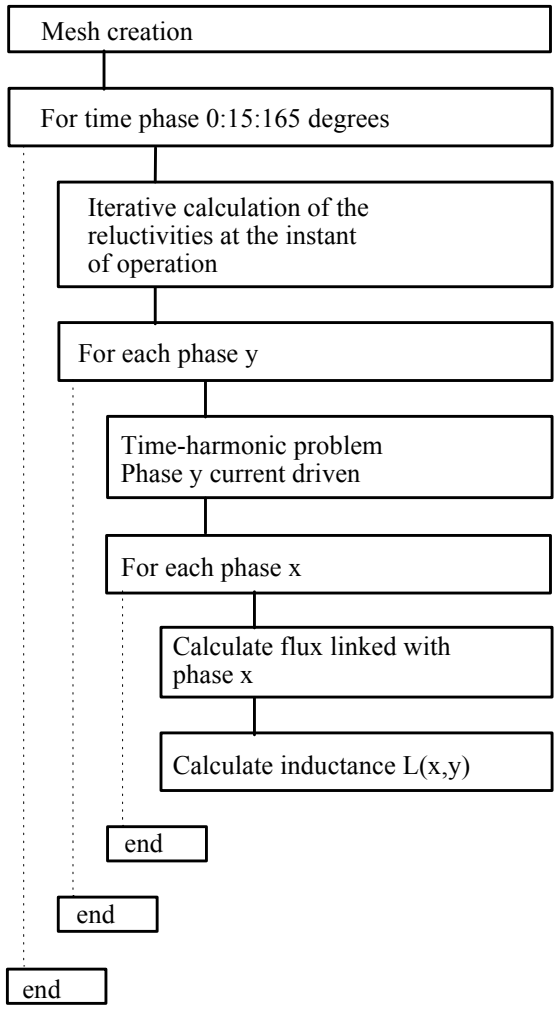

Figure 3 : 2D-FEM calculation of the motor parameters

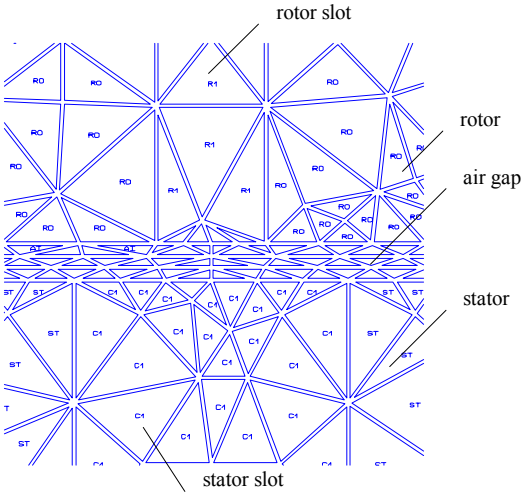

Figure 4 : Detail of the mesh

To take simultaneously into account both time-harmonic effects and saturation, an iterative finite element method is implemented [4]. A time-harmonic solver is applied to calculate eddy currents in the rotor bars. Starting from the current distribution in the machine a magnetostatic solution calculates the saturation level. Both at the real and imaginary instant of excitation, the reluctances of the iron are known. Making a combination of those two values, a kind of average reluctance can bring up a description of the saturation level of the machine. This value can be used to come to one solution for the whole time period [4]. However, when simulating motor behaviour, the evolution in time of the motor parameters is investigated. For this purpose, the iterative finite element calculation can be done with only the real solution of the magnetic field. The reluctivities obtained from the last nonlinear static solution are assumed to be the reluctivities that describe the saturation level in the machine at the concerned instant of time.

4.2.Inductance matrix

At each time step, nine linear independent time-harmonic problems are defined, each by applying a known current to one phase. The other phases are open. The time-harmonic calculation is performed with the previous obtained reluctivities. For each of the nine problems, the fluxes through all nine phases are calculated. The mutual inductance of phase x with the excited phase y is

$$L = \frac{N_x \cdot \phi_x \cdot \ell}{I_y} \qquad (5)$$

with N_x the number of turns of phase x, ϕ_x the flux through phase x, ℓ the length of the machine and I_y the excitation current of phase y.

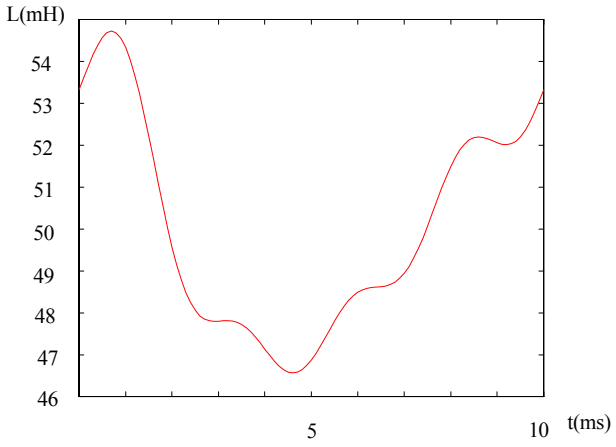

Figure 5 : Variation of the self inductance of the first stator phase

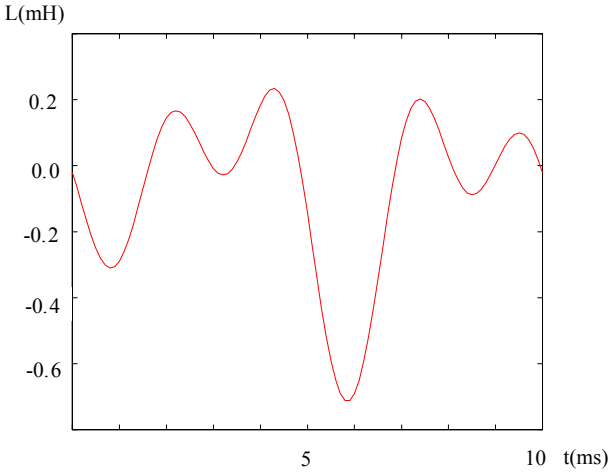

Figure 6 : Variation of the mutual inductance of a stator and a rotor phase.

Defining a rotor phase as one rotor bar gives rise to a problem when looking to the flux linked with this phase. In order to avoid this difficulty, an intermediate definition of rotor phases is used : phases A to E are defined as the series connections of two successive rotor bars, phase F is defined as the series connection of the first and the last rotor bar. The relation between the voltages is

$$[U_\bullet] = [C].[U_r] \qquad (6)$$

or fully written

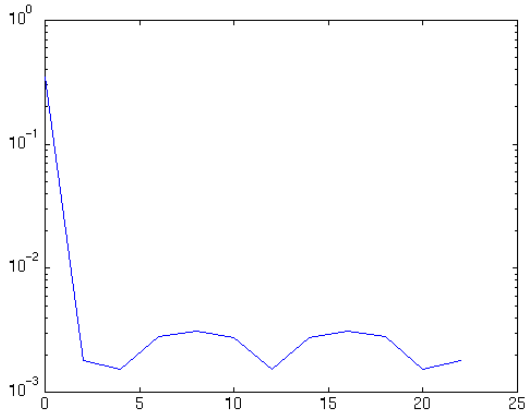

Figure 7 : Fourier spectrum of the self-inductance of a stator phase

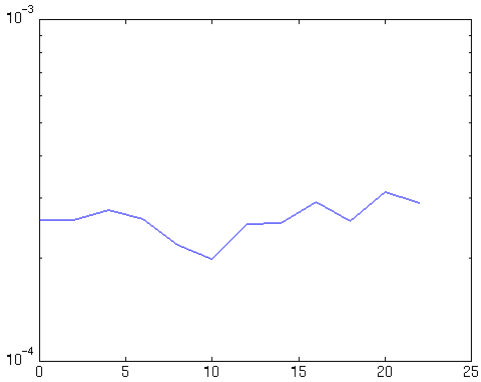

Figure 8 : Fourier spectrum of the mutual inductance between a stator and a rotor phase

$$\begin{bmatrix} U_A \\ U_B \\ U_C \\ U_D \\ U_E \\ U_F \end{bmatrix} = \begin{bmatrix} 1 & -1 & 0 & 0 & 0 & 0 \\ 0 & 1 & -1 & 0 & 0 & 0 \\ 0 & 0 & 1 & -1 & 0 & 0 \\ 0 & 0 & 0 & 1 & -1 & 0 \\ 0 & 0 & 0 & 0 & 1 & -1 \\ 1 & 0 & 0 & 0 & 0 & 1 \end{bmatrix} \cdot \begin{bmatrix} U_1 \\ U_2 \\ U_3 \\ U_4 \\ U_5 \\ U_6 \end{bmatrix} \qquad (7)$$

The inductance matrix of the rotor phases A..F, $[L_\bullet]$, can be converted to the inductance matrix of the original defined rotor phases, $[L_r]$, by

$$[L_r] = [C]^{-1} \cdot [L_\bullet] \qquad (8)$$

A comparison with analytical and measured data is given in table 1.

4.3. Fourier series of the inductance matrix

The fundamental frequency of the time varying inductance matrix is twice the fundamental excitation frequency. One period of variation of the inductance values is shown in figures 5 and 6. The inductance matrices for each time step are decomposed in 12 components using a Fast Fourier Transform (FFT) algorithm. The spectrum of the self inductance of a stator phase is shown in figure 7. The spectrum of the mutual inductance between a stator phase and a rotor phase is shown in figure 8.

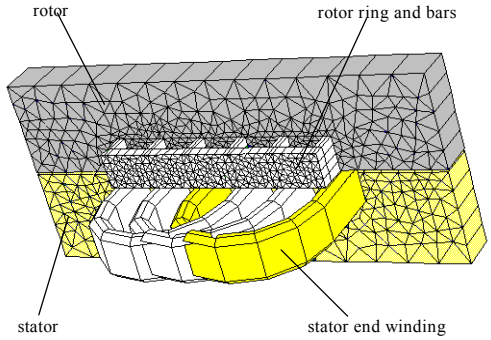

Figure 9 : Three-dimensional Finite Element Model of a side of a linear induction motor

	Measured (mH)	Analytical (mH)	Computed (mH)	Fundamental (mH)
L_{S1}	25.1	25.4	30.2	28.8
$M_{S1,S2}$	-12.9	-14.4	-16.0	-14.6
$M_{S1,S3}$	2.00	3.39	3.13	3.30
$M_{S1,R1}$	0.168	0.203	0.205	-0.015
$M_{S1,R2}$	0.019	0.034	0.123	-0.035
$M_{S1,R3}$	-0.133	-0.136	-0.119	-0.121
$M_{S1,R4}$	-0.285	-0.305	-0.270	-0.261
$M_{S1,R5}$	-0.231	-0.254	-0.225	-0.206
$M_{S1,R6}$	-0.182	-0.203	-0.210	-0.193

Table 1: Comparison between measured, analytical obtained and computed data.

5. 3D FINITE ELEMENT CALCULATION OF THE END EFFECTS

5.1. Calculation of the stator and rotor ring end effects

To consider the stator and rotor end effects, a real three-dimensional finite element model is required. The geometry of the end windings and the stator and rotor yoke is shown in figure 9.

The following inductances must be calculated: self inductance of the stator end windings and the rotor end ring segments, mutual inductances between stator end

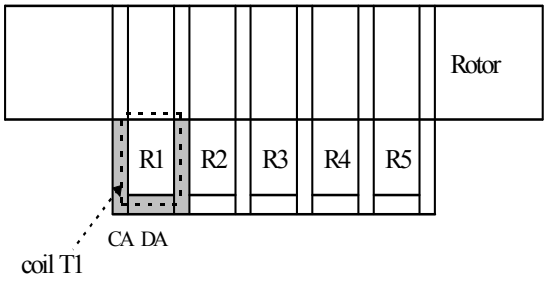

Figure 10 : Rotor end ring segments

windings and the rotor end ring segments. The five rotor end ring segments R1 to R5 are defined as in figure 10.

5.2. Calculation of the self inductances

There are two ways to obtain the inductance values from the solution of the magnetic field: stored magnetic energy and flux linkages.
Using the first method, the total magnetic energy stored in the end winding area is calculated. The inductance value obtained in this way is strongly influenced by the stray field near the air gap of the linear induction motor (figure 11). From figure 12, one can also see that there is a concentration of magnetic energy in the iron yoke near the border.

To calculate the inductances from the flux linkages with the stator end windings or the rotor end ring, the magnetic flux density has to be integrated over the surface of the end winding or the end ring segment. The integration surface is taken on the side of the end winding or the end ring whichever is closest to the air gap. The value obtained this way has almost no contribution of the stray field near the air gap. It is the inductance value according to this definition that can be measured in practice.

5.3. Calculation of the mutual inductances

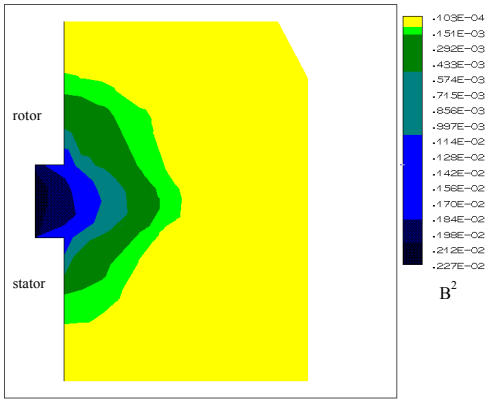

Figure 11 : stray field near the air gap

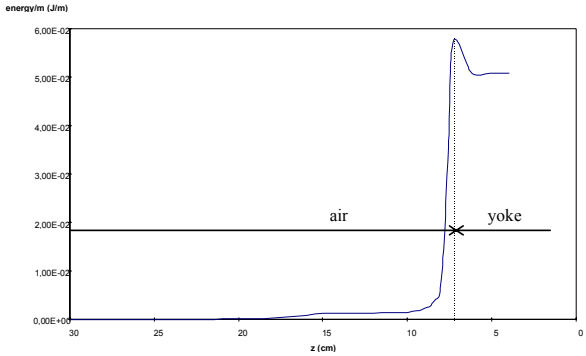

Figure 12 : energy density as a function of place

Again, the inductance values can be obtained using the flux linkages with a winding, here caused by currents in another winding.

Also the induction principle can be used to determine the mutual inductances. The method here is described for the mutual inductance between a stator end winding and a rotor end ring segment. The stator coil is excited with an ac current. In the problem definition, the rotor segment is given a high resistivity and is short-circuited on the border of the iron yoke with coil T1 (figure 10). From the current induced in this coil, the inductance value can be calculated taking into account that the induced current and the self inductance of the rotor end ring are very small, so that the flux from the induced current is negligible.

5.4. Comparison of measurements and results

To measure the desired values of self and mutual inductances, measuring coils fixed to the end windings and the ring segments are used. The appropriate winding is excited and from the induced voltage in the measuring coil, the inductance value can be obtained. A comparison between computed and measured data is given in table 2.

	Computed ($*10^{-3}$ mH)	Measured ($*10^{-3}$ mH)
L_{S1}	331	315
$M_{S1,S2}$	-193	166
$M_{S1,S3}$	43	40
L_{R1}	0.050	0.051
$M_{S1,R1}$	3.83	3.37
$M_{S1,R2}$	4.22	3.57
$M_{S1,R3}$	3.95	3.34
$M_{S1,R4}$	-1.25	-1.05
$M_{S1,R5}$	-1.42	-1.50

Table 2: Comparison between computed and measured data

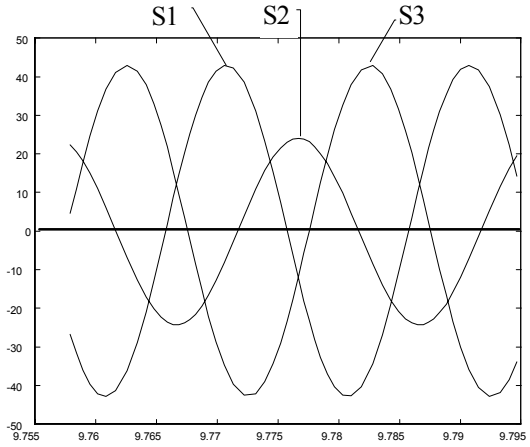

Figure 13 : steady state stator currents

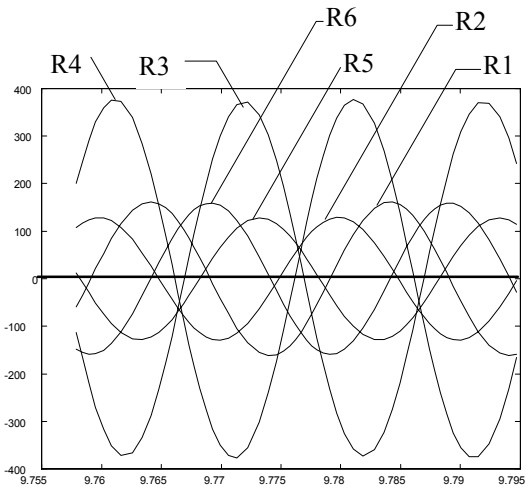

Figure 14 : Steady state rotor currents

L and M indicate the self and mutual inductances respectively, the indices with "S" are for the stator end windings and with "R" for the rotor end ring segments. The calculated values come from the flux linkages. There is no physical method to measure the total magnetic energy in the end winding area.

6. DYNAMIC BEHAVIOUR OF THE LINEAR MOTOR

The rotor bars of the linear induction motor are at both ends short-circuited by the end ring. Stator windings are Y-connected. Therefore, the equation system is reduced to seven equations. No motion is considered.

6.1.Linear steady state behaviour

The set of linear first order differential equations can be solved by an ordinary differential equations (ODE) algorithm. A simulation of the steady state behaviour is shown in figure 13 and figure 14. The linear motor is a geometric asymmetric induction motor. The current through the second stator winding is smaller than the current through the first and the third winding. A neutral point voltage variation at 50 Hz is observed. The rotor bars are two by two symmetric.

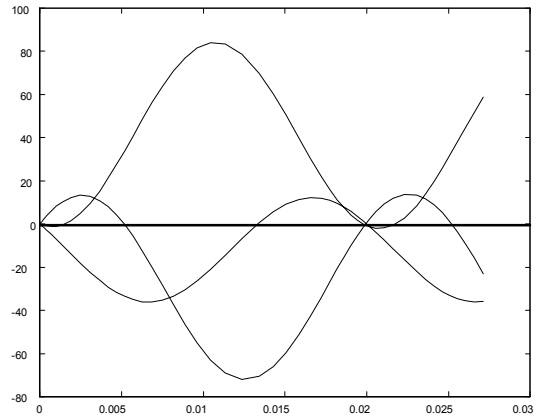

Figure 15 : Transient starting stator currents

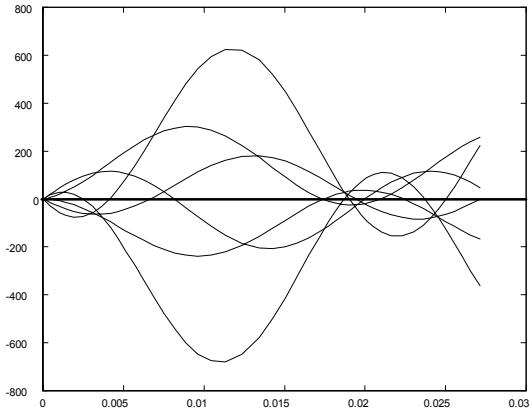

Figure 16 : Transient starting rotor currents

6.2. Transient phenomena of starting

Looking to the eigen values of the system matrix of the linear system, the stability and the dynamic behaviour of the system can be proved (table 3).

In figures 15 and 16 the transient currents for start are shown. For a large number of periods the phases have the same zero crossing. The time constant of the stator current DC offset is seen to be in the range of a second, a value that is confirmed by the last two eigen values. The time constants of the rotor currents depend on the first five eigen values. As can seen from the zero

Table 3 : Eigen Values

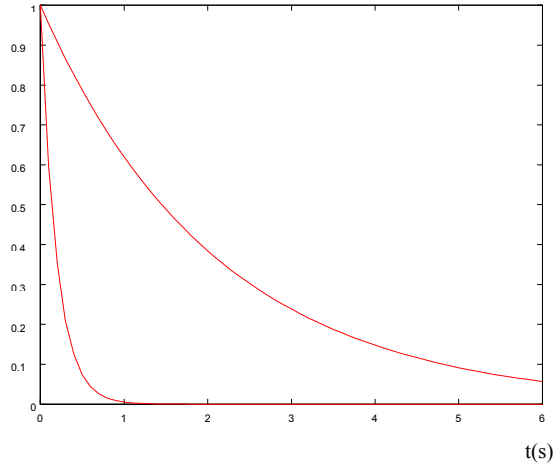

Figure 17 : Exponential damping of the DC offset of the current

1	2	3	4	5	6
-16.23	-49.19	-15.91	-13.67	-0.94	-14.33
-13.49	-23.26	-13.21	-11.34	-0.48	-12.82
-10.92	-14.54	-10.64	-8.84	-8.27E-05	-6.64
-5.22	-12.57	-5.11	-4.36	-4.66E-05	-2.33
-2.25	-10.69	-2.19	-1.80	-3.70E-05	-0.94
-0.94	-0.79	-0.91	-0.76	-3.21E-05	-0.48
-0.48	-0.39	-0.47	-0.39	-3.14E-05	

1	without end effects, symmetrizised
2	with end effects
3	with end effects, symmetrizised
4	with ten times the end effects
5	with extra rotor ring impedances
6	third rotor bar broken

crossings of the transient stator and rotor currents, the DC component of the rotor currents decays much faster (figure 17).

6.3. Nonlinear steady state behaviour

Figures 18 and 19 show stator and rotor currents in a highly saturated linear induction motor. The shapes of the currents are no longer sinusoidal. Some numerical difficulties are encountered when high saturation levels are taken into account.

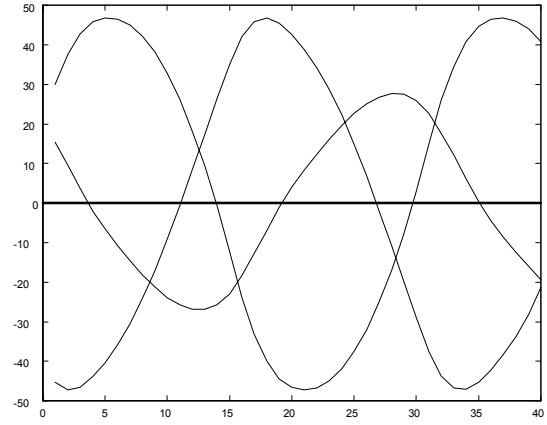

Figure 18 : Stator currents of the saturated linear motor

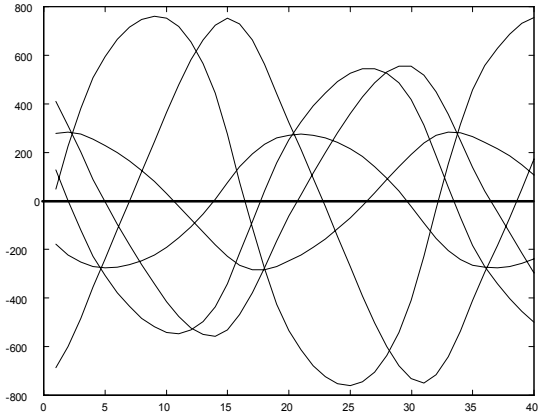

Figure 19 : Rotor currents of the saturated linear motor

6.4. Nonlinear steady state behaviour regarding raised end effects

The amplitudes of the currents change marginally when applying extra end inductances to the model. The most interesting effect is obtained when increasing rotor end ring resistance. The currents through the rotor bars become smaller. The currents through the bars at both ends of the rotor are smaller in comparison with the currents through the middle rotor bars (figure 20).

6.5 Steady state behaviour with a broken rotor bar

The steady state behaviour of the motor with a broken rotor bar is simulated. The effect on the stator side is minimal. The effect on the rotor currents is that the currents in the non-broken rotor bars try to balance the missing rotor current (figure 21).

6. CONCLUSIONS

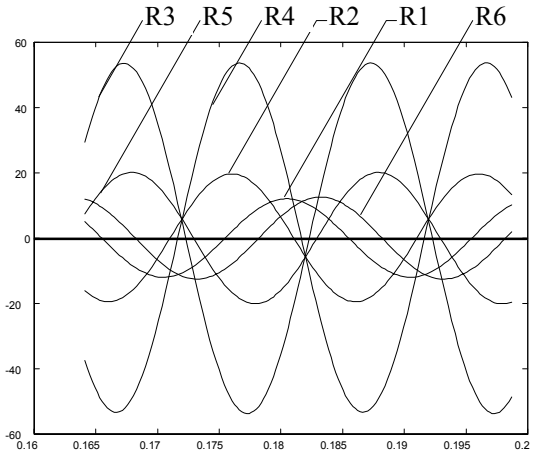

Figure 20 : Rotor currents of the linear motor with raised rotor ring impedances

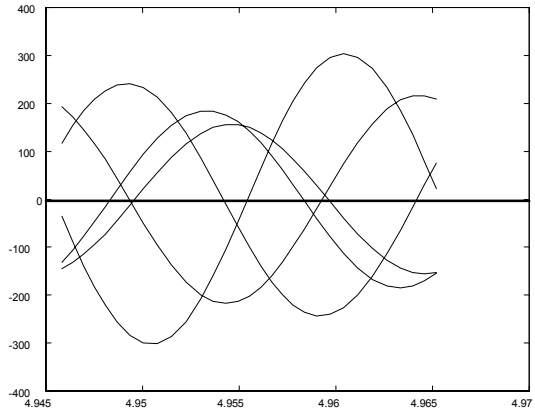

Figure 21 : Rotor currents in rotor with one rotor bar broken

The advantage of using a linear induction motor model is the possibility of easy comparison of the calculation methods to both analytical formulae and measurements. For evaluating induction motor behaviour, the linear motor provides the opportunity to change in a non-destructive way the configuration of stator windings, rotor bars, rotor end rings and external circuits. Simulation of the induction motor behaviour, both numerical and practical is possible for almost every situation. A linear motor can also be used for studying stator and rotor end effects. A disadvantage of the linear motor is the difficulty of taken motion effects into account.

7. ACKNOWLEDGEMENTS

The authors are indebted to the Belgian Ministry of Scientific Research for granting the project IUAP No. 51 on Magnetic Fields.

8. REFERENCES

[1] Lowther, D.A., Forghani, B., Freeman, E.M., *A Benchmark Model for Comparing Induction Machine Analyses*, Proc. Compumag 1995, pp. 154-155.

[2] Laithwaite, E.R., *Induction machines for special purposes*, Newnes, London, 1966.

[3] Forsythe, G.E., Malcolm, M.A., Moler, C.B., *Computer Methods for Mathematical Computations*, Prentice-Hall, 1977.

[4] De Weerdt, Robrecht, *Eindige elementen modellering van kooianker inductiemotoren*, Ph.D. Thesis, Leuven, 1995.

[5] De Weerdt, R., Hameyer, K., Belmans, R., *End ring inductance of a squirrel-cage induction motor using 2D and 3D finite element methods*, Proc. Conf. IAS Annual Meeting, Orlando, Oct. 1995, pp. 515-522.

[6] Nürnberg, W., *Die Asynchronmaschine*, Springer-Verlag, Berlin, 1965.

[7] Lowther, D.A., Silvester, P.P., *Computer-Aided Design in Magnetics*, Springer-Verlag, Berlin, 1985.